Bio-mimic Ti-Ta composite with hierarchical “brick-and-mortar” microstructure

Xu, Shenghang; Du, Meng; Li, Jia; Yan, Kun; Cai, Biao; He, Quanfeng; Fang, Qihong; Magdysyuk, Oxana; Liu, Bin; Yang, Yong; Liu, Yong

DOI:
10.1016/j.mtla.2019.100463

Document Version
Peer reviewed version

Citation for published version (Harvard):
Xu, S, Du, M, Li, J, Yan, K, Cai, B, He, Q, Fang, Q, Magdysyuk, O, Liu, B, Yang, Y & Liu, Y 2019, 'Bio-mimic Ti-Ta composite with hierarchical “brick-and-mortar” microstructure', *Materialia*, vol. 8, 100463.
https://doi.org/10.1016/j.mtla.2019.100463

Bio-mimic Ti-Ta Composite with Hierarchical "Brick-and-Mortar" Microstructure

Shenghang Xu[1], Meng Du[1,2], Jia Li[3], Kun Yan[4], Biao Cai[5*], Quanfeng He[2], Qihong Fang[3], Oxana Magdysyuk[6], Bin Liu[1], Yong Yang[2,7*], Yong Liu[1*]

[1]. State Key Laboratory of Powder Metallurgy, Central South University, Changsha 410083, PR China

[2]. Department of Mechanical Engineering, College of Engineering, City University of Hong Kong, Kowloon Tong, Kowloon, Hong Kong, China

[3]. State Key Laboratory of Advanced Design and Manufacturing for Vehicle Body, Hunan University, Changsha, 410082, PR China

[4]. School of Materials, University of Manchester, Manchester, M13 9PL, UK

[5]. School of Metallurgy and Materials, University of Birmingham, Birmingham, B15 2TT, UK

[6]. Diamond Light Source Ltd, Harwell Science and Innovation Campus, Didcot, OX11 0DE, UK

[7]. Department of Materials Science and Engineering, College of Engineering, City University of Hong Kong, Kowloon Tong, Kowloon, Hong Kong, China

Abstract: Nature materials, such as bones and nacre, achieve excellent balance of toughness and strength via a hierarchical "brick-and-mortar" microstructure, which is an attractive model for engineering materials design. Here, we produced nacre-like Ti-Ta metallic composites via a powder metallurgy process, during which mixed powders were sintered by spark plasma sintering, followed by hot and cold rolling and then annealing. The structure consists of soft Ta-enriched regions and hard Ti-enriched regions in a hierarchical and laminated fashion. The microstructural heterogeneity spans several scales due to the diffusion between Ti and Ta. This yields a novel metal-metal composite with a balanced combination of strength and ductility (1226 MPa ultimate tensile strength and 20.8% elongation), outperforming most of conventional Ti based alloys and composites. Via the complementary in situ synchrotron X-ray diffraction and electron microscopies, it is found out that multiple micromechanisms are active, including nano-particle and dislocation localized

strengthening as well as phase transformation induced plasticity. The manufacturing route developed here is versatile, capable of making high performance bio-mimic metallic composites.

Keywords: bio-mimic materials; metal-metal composites; Ti-Ta; microstructure

Corresponding authors:

Email: yonliu@csu.edu.cn (Yong Liu); yonyang@cityu.edu.hk (Yong Yang); b.cai@bham.ac.uk (B.Cai)

1. Introduction

Metal matrix composites (MMCs) always provide a magnificent playground for broadening the utilization of metals, owing to the desirable mechanical properties and potential applications which are inaccessible for pure metals [1, 2]. Generally, the strength of MMCs can be obviously improved through adding hard ceramic particles [3, 4] or enhanced fibers [5, 6], which may also compromise ductility and toughness. Such strategy usually leads to the catastrophic and unpredictable failure in service process. Therefore, optimizing combination of strength and toughness comes as an ongoing research topic for designing high performance MMCs.

Nature materials provide distinctive ideas for achieving high performance materials, which are always composed of limited components accompanied by excellent mechanical properties, such as high strength and toughness, benefited through hierarchically ordered structure at multi-scale levels [7-9]. The special structure and the distinguished properties are chased by scientists, and thus, bio-mimic materials start to come into being in recent decades. The most studied model among these natural materials is the nacreous structure in some mollusk shells, consisting of aragonitic ($CaCO_3$) and organic materials, which is better named as "brick-and-mortar" structure [10, 11]. The brittle aragonitic provides high strength and hardness while the organic materials possess excellent toughness and crack-resistance, and these integrated factors lead to outstanding properties of both excellent strength and toughness, which are mutually exclusive in most manufactured materials. Therefore, more and more studies are focused on optimizing the micro/nanostructures of now available materials. For example, Motomichi [11] has fabricated hierarchical metastable nano-laminated steels with superior crack resistance, inspired by the structure of human bones.

However, the fabrication of bulk biomimetic materials with organized structures is by no means a low-hanging fruit, owing to the tough challenges: how to better combine the organized hierarchical structure and the efficiency. Nowadays, various methods are utilized to fabricate nacre-inspired MMCs, such as layer-by-layer [12, 13], self-assembly [14, 15], freeze-casting [16, 17], electro-phoretic deposition [18], and vacuum evaporation [19]. However, the homogeneous distribution and alignment of "brick" in metal matrix cannot be achieved with great ease, because of intrinsic differences between hard "brick" and soft "mortar", such as agglomeration as well as density discrepancy. Besides, the weak combination between "brick" and "mortar" may deteriorate the mechanical properties, which is ubiquitous for MMCs.

In order to obtain a high performance nacre-inspired “brick-and-mortar” structured MMCs, the alternating arrangements of hard and soft phases must be properly assembled, and the bonding between adjacent components should be strong enough. Here, we propose a convenient and effective technique to fabricate Ti-Ta “brick-and-mortar” structured bulk through a powder metallurgy process. Thereinto, Ti-enriched bands act as “brick” and Ta-enriched bands are regarded as “mortar”. Attributed to this bio-inspired structure, the Ti-Ta composite exhibits strong-yet-ductile properties, and this provides an effective strategy for designing and fabricating novel high-performance MMCs.

2. Experimental

2.1 Material preparation

The elemental powder of Ti (particle size< 30 μm, purity> 99.9%) and 20% atom fraction of Ta powders (particle size< 5 μm, purity> 99.99%) were blended by a jar mill for a period of 4 h. The SPS process was applied at 1200 ºC for 5 min by using a HP D 25/3 Spark Plasma Sintering System. The pressure was 40 MPa, the heating rate was 200 ºC/min and the cooling rate was 50 ºC/min. The shape of the composites produced by SPS was cylindrical with a diameter of 40 mm and a height of 6 mm. Subsequently, the composites were heated in a furnace at 700 ºC for 30 min and rolled (referred to as ‘as-rolled’ hereafter). The composites underwent a height reduction of 0.5 mm for each rolling pass, were reheated in the furnace for 1 min before the next rolling pass and air cooled for the last rolling pass. A total height reduction of 85% was achieved after the rolling. Finally, the as-rolled composites were annealed in the furnace at 600 ºC for 30 min (referred to as ‘as-annealed’ hereafter) followed by water quenching. The schematic diagram of the material preparation is shown in Fig.1.

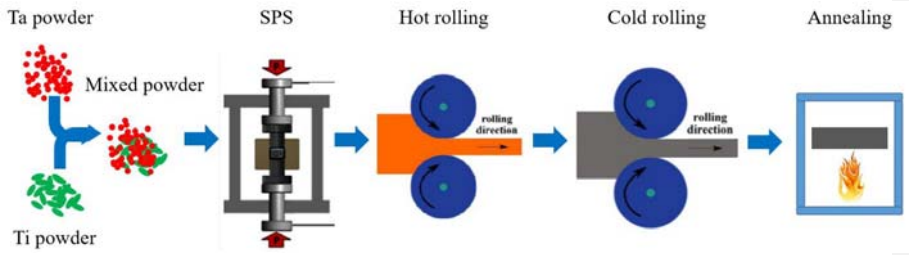

Fig.1 The diagrammatic sketch of the processing of the Ti-Ta composite.

2.2 Characterization

The microstructures were examined by using an FEI Nova Nano250 scanning electron microscope (SEM) equipped with an energy dispersive X-ray analyzer (EDX). The TEM samples were electro-polished with an electrolyte of 6% perchloric acid, 60% methanol and 34% n-butyl alcohol (in volume) at a temperature of 243 K. TEM observations were performed using an FEI Tecnai 20 transmission electron microscope under an accelerating voltage of 200 kV. The phase identification was performed on bulk samples using an X-ray Diffraction analyzer (Rigaku Rapid IIR) with a Cu Kα radiation operated at 45 kV at room temperature.

The tensile composites were machined by wire-electrode cutting from the as-rolled and as-annealed composites along the rolling direction. The tensile tests and the loading-unloading-reloading tests were both conducted at a strain of 5×10^{-2} s^{-1} at room temperature using an 858 Mini Bionix II machine with an extensometer.

The in-situ tension samples were prepared by using FEI Scios focused ion beam/scanning electron microscope (FIB/SEM). The in-situ tension test was performed in transmission electron microscope operating under 200 kV (TEM, JEOL 2100F) equipped with the Hysitron PI 95 TEM PicoIndenter. The displacement rate was 3nm/s.

2.3 Synchrotron radiation experiment

The synchrotron radiation experiments were conducted at the high energy beam line- I12 at the Diamond Light Source~~ID15B of the European Synchrotron Radiation Facility~~, with an incident X-ray energy of 53 ~~86.94~~ keV. The RF Pixium 4343 2D area detector with a pixel size of 148 μm × 148 μm was used in transmission mode. The uniaxial tensile test was performed at ambient temperature at a constant strain rate of 1×10^{-4} s^{-1} to failure~~a final true strain~~.

3. Results

3.1. Microstructures

Fig.2 shows the microstructures of as-rolled and as-annealed composites. As seen in Fig.2(a), the Ta-enriched bands (brighter region), acted as “mortar”, exhibit an elongated fiber-like microstructure and are uniformly distributed inside the composite. Very few pores can be detected after rolling. The Ti-enriched band structure, served as ‘brick’, consists of a

high-density of α phase (Fig. 2c). The thickness of the Ta-enriched band is approximately 5 μm, while that of the Ti-enriched band is above 10 μm. The α phase in Ti-enriched band conforms to a Widmanstatten structure, and has a width of ~150 nm, as shown in the TEM image of Fig.2(c). Fig. 2(d) shows the TEM image of the Ta-enriched band. Due to the combined effects of solid solution and elemental distribution between Ti and Ta, two different regions can be identified inside the Ta-enriched band, one rich in Ti (named "R-Ti" thereafter) and the other rich in Ta (named "R-Ta"). The size of both R-Ti and R-Ta is less than 1 μm. After short-time annealing (600 ^{o}C for 30 min), no obvious change can be found in the Ti-enriched band with a similar Widmanstatten structure (Fig.2(f)), while the size of the Ta-enriched band remained almost unchanged, but its inner microstructure was changed remarkably. As shown in Fig.2(g), a plenty of needle-like nano-precipitations can be observed inside R-Ta with a length of ~100 nm and a width of ~10 nm. The nano-precipitations inside R-Ta are rich in Ti and thus named as "Ti-rich nano-precipitate" hereafter. The chemical composition of R-Ti and R-Ta is shown as the Table in Fig.2. Fig.2(h) shows the HRTEM image of the interface between the nano-sized Ti rich phase and the R-Ta matrix phase. It is interesting to note that the Ti-rich nano-precipitate presents a coherent interface with the R-Ta matrix, shown as the IFFT images in Fig. 2(i). Besides, the Ti-rich

nano-precipitate and the R-Ta matrix are both of body centered cubic (bcc) structure. After annealing, few dislocations can be observed.

Fig.2 (a-d) The images of the as-rolled Ti-Ta composite: (a) the SEM image along the transverse direction; (b) large magnification of Ti-enriched and Ta-enriched bands; (c) the Ti-enriched band of Widmanstatten α phase with corresponding selected area electron diffraction (SAED) patterns on the right; (d) the Ta-enriched band consists of R-Ti and R-Ta with corresponding FFT image on the right; (e-i) the images of the as-annealed Ti-Ta composite: (e) the SEM image of the Ti-enriched and Ta-enriched bands; (f) the Ti-enriched band; (g) the Ta-enriched band; (h) The HRTEM image of the Ti-rich phase in R-Ta; (i) The IFFT image of the interface between Ti-rich phase and R-Ta in (h).

3.2. Mechanical properties

Fig. 3(a) shows the representative engineering stress-strain curves of the as-rolled and as-annealed Ti-Ta metal-metal composites. After annealing, the ductility of the composite improves from 13.2% to 20.8%. Interestingly, although the yield stress of the as-annealed composite is slightly lower (950 MPa) than that of the as-rolled (998 MPa), the ultimate tensile strength increases from 1108 MPa to 1226 MPa. This is in stark contrast to most alloys, which when show ductility improvement, the strength usually ~~reduce~~reduces (so called 'ductile-strength trade-off'). From the stress strain curves, the strain hardening rate was

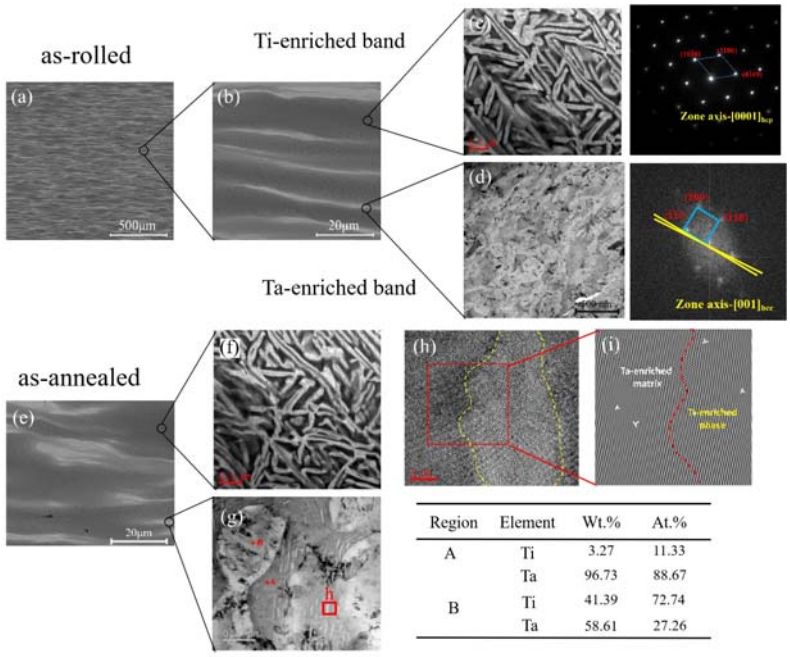

Region	Element	Wt.%	At.%
A	Ti	3.27	11.33
	Ta	96.73	88.67
B	Ti	41.39	72.74
	Ta	58.61	27.26

calculated for the as-rolled and as-annealed composites. As seen in Fig.3(b), the strain hardening effect is initially lower in the as-annealed composite than in the as-rolled composite for low plastic strains; however, it decreases with the increasing flow stress more slowly in the as-annealed composite than in the as-rolled one. Besides, the true stress- strain curves of both composites are shown in the inset image of Fig.3(b). As a result, the strain hardening effect in the as-annealed composite becomes higher than that in the as-rolled composite for high plastic strains. It ~~Besides, it~~ is worth mentioning that the as-annealed composite also shows an up-turn in the strain hardening rate. This phenomenon of strain hardening rate was previously observed in heterogeneous laminated materials, such as in the Ti alloy with both ultrafine- and coarse-grain lamellae and copper-bronze heterogeneous laminate [2, 8]. Fig. 3(c) shows the comparison of our annealed Ti-Ta composites with a variety of Ti alloys [20-42] in terms of their UTS and tensile ductility. Evidently, our Ti-Ta composite shows a much better combination of strength and ductility, outperforming most of others reported hitherto in the literatures.

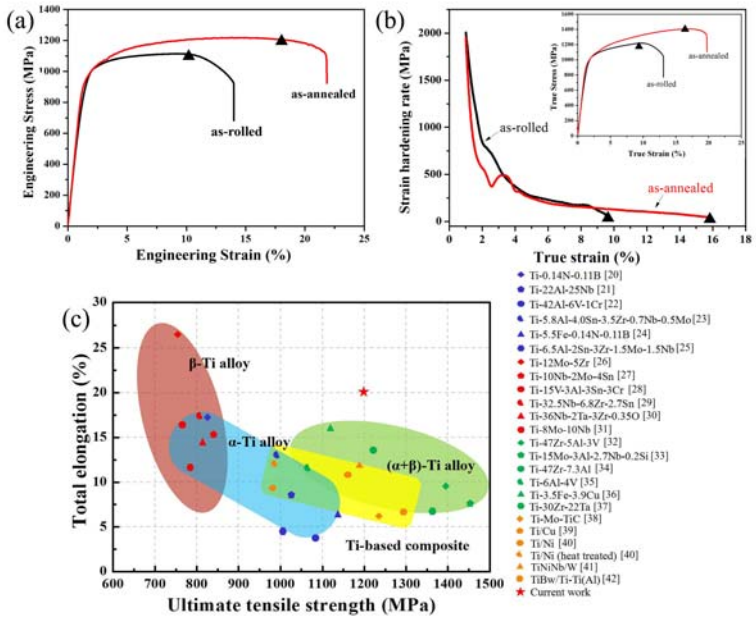

Fig.3 Tensile properties of Ti-Ta composite. (a) The engineering stress-strain curves; (b) the strain hardening rate curves of the Ti-Ta metal-metal composites at room temperature inset with the true stress-true strain curves; (c) The strength and ductility of the present Ti-Ta composite compared with other Ti alloys [20-42].

To~~–~~ study the back-stress effect~~probe the inter-phase interactions at the macroscopic scale~~, we conducted the loading-unloading-reloading tests on the as-annealed bulk composite, and the curves are presented in Fig.4(a). The hysteresis loop formed during the unloading-reloading cycle signals an obvious back stress effect [43, 44]. Following the procedure in Ref.[43], we calculated ~~backed out~~ the back stress at different plastic strains. As shown in Fig. 4(b), the back stress increases with the plastic strain, and reaches 756 MPa at the strain of 7.2%. This back-stress effect is significant and increases as the plastic flow continues, which implies that dislocation movements became hindered in our composites after annealing.

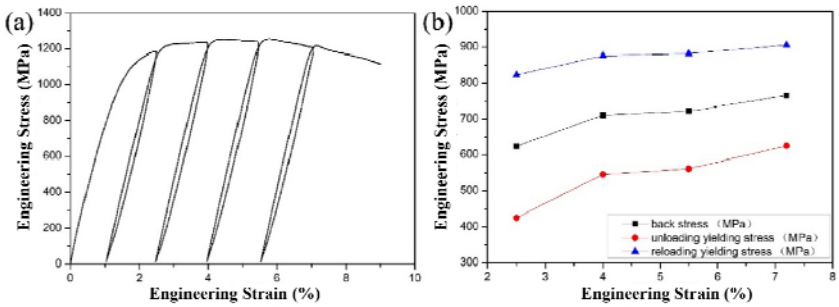

Fig.4 (a) The loading-unloading-reloading curve of the as-annealed samples at room temperature; (b) the values of back stress, unloading yielding stress and reloading yielding stress at different engineering strain.

To understand the mechanisms underlying the strength-ductility synergy in our as-annealed Ti-Ta composite, the strength of the individual Ti- and Ta-enriched band was measured through in-situ tensile test in a SEM. Fig.5(a) shows the tensile samples prepared by FIB milling in the Ti- and Ta-enriched band, respectively. From Fig.5(b), it can be seen that the yield strength is about 920 MPa and the ultimate tensile strength is 1172 MPa for the Ti-enriched band while 875 MPa and 1138 MPa for the Ta-enriched band. Interestingly, both properties are considerably lower than those of the bulk Ti-Ta composites. Besides, the Ti-enriched region exhibited limited ductility after yielding without appreciable strain hardening, which can be attributed to the difference of mechanical properties between α phase and β phase. The β phase with a BCC structure is more ductile than α phase, leading to the occurrence of plastic instability. As for the Ta-enriched region, the stress rise and fall repeated during the tensile process. It can be explained by the stress-induced martensite transformation, which will be discussed later. This is in sharp contrast to the behavior of the bulk Ti-Ta composites, which suggests that the strength-ductility synergy as witnessed in the bulk sample should originate from the mechanistic interaction of the Ti- and Ta-enriched bands.

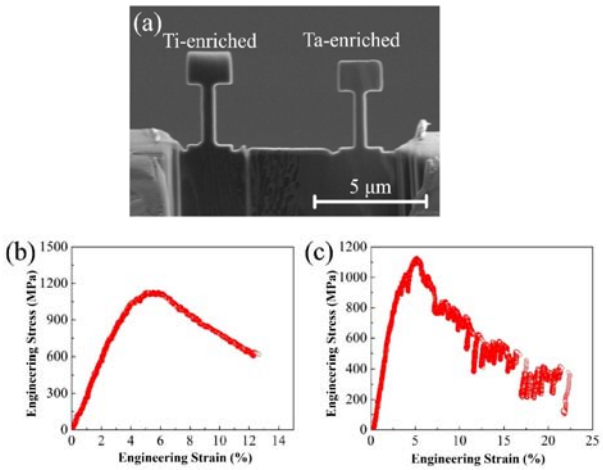

Fig. 5 (a) The SEM image of the in-situ tensile samples (as-annealed) fabricated through FIB; (b) and (c) The engineering stress-strain curves of the Ti-enriched and Ta-enriched bands by in-situ tensile tests, respectively.

The nano-indentation tests across the Ta-enriched band were applied on as-rolled and as-annealed composites before and after tensile deformation, as shown in Fig.6. In Fig.6(b), four lines mean the microhardness across the Ta-enriched bands, and the "before" and "after" mean the microhardness of composites before and after tensile deformation. It shows that Ti-enriched band is harder than the Ta-enriched band in both the as-rolled and as annealed conditions. Additionally, the microhardness of Ta-enriched bands (~330 MPa) reaches almost the same as that of Ti-enriched bands (~350 MPa) for as-annealed composite.

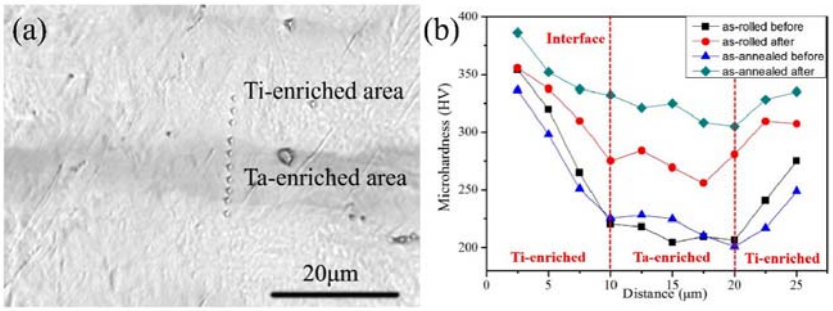

Fig.6 (a) The optical image of the testing zone; (b) line distribution of microhardness of different Ti-Ta composites.

Fig.7 shows the TEM images of Ti-Ta composite after tensile deformation. In Ti-enriched bands, a high density of dislocations can be distinguished clearly. As for the Ta-enriched bands, it is interesting that the dislocations are more likely to pile up and accumulate inside the Ta-rich region (R-Ta) other than Ti-rich region (R-Ti), as shown in Fig.7(b). Moreover, a high density of dislocations can be seen in both the Ti-rich phase and the R-Ta phase according to the HRTEM image [Figs. 7(c-d)]. These results indicate that the high density Ti-rich nano-precipitates promote dislocation pile-up and accumulations inside R-Ta.

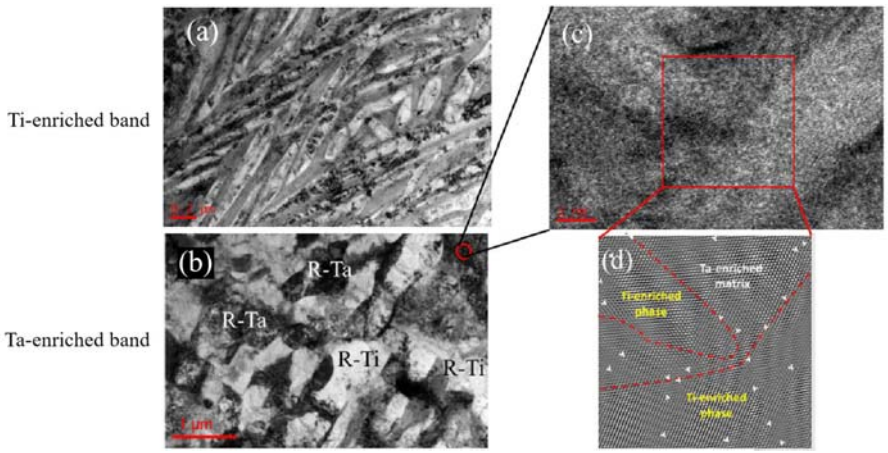

Fig.7 TEM images of the as-annealed composites after tensile deformation: (a) Ti-enriched band; (b) Ta-enriched band; (c) The HRTEM image of the Ti-rich phase in R-Ta and (d) The IFFT image of the interface between Ti-rich phase and R-Ta in (c).

It is well known that stress induced martensitic phase transformation (SIMT) can also mediate plasticity in titanium alloys [45, 46]. In our previous work [47], martensitic transformation only happened when the content of Ta varied from 15 to 28 at%, and the composition of R-Ti is right located in this region. Therefore, we ~~also~~ performed in situ tensile tests under synchrotron radiation to check if phase transformation occurred during the tensile deformation process. Fig.8(a) shows the diffraction curves obtained along the loading direction. It is interesting to note that α" martensitic phases formed when the strain reached up to 7.5%. Indeed, martensitic phases could be observed after the deformation, as seen in Fig. 8(b). According to the selected area electron diffraction pattern (SAED) [Fig. 8(c)] obtained from the circled area in 8(b), the orientation relationship (OR) between the β matrix and martensitic α" phase can be identified as $[111]_{\beta}//[110]_{\alpha''}$. It is well accepted that SIMT improves ductility by increasing the flow stress in a localized area to restrain the plastic

instability [48, 49]. Based on the above considerations, we believe that the annealing induced strength-ductility synergy observed on our Ti-Ta composite is mainly due to an enhanced back stress effect in a "brick and mortar" microstructure, ~~with~~ nano-sized precipitation hardening~~s~~ and the SIMT effect.

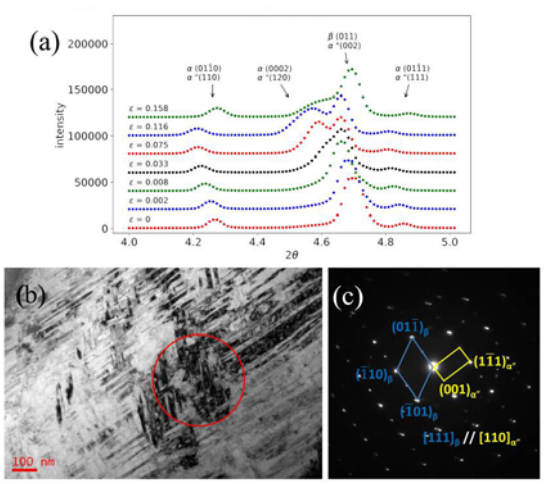

Fig.8 The synchrotron radiation curves of the as-annealed samples during the tensile deformation through loading direction; (b)The bright field image of stress-induced martensitic phase in R-Ta; (c) The corresponding selected area electron diffraction (SAED) patterns of martensitic phase (α″) in (b).

4. Discussion

~~4.1 Back stress effect~~

For many materials, annealing process may lead to the decrease of dislocation density, and thus, decrease the yield strength. As for ~~this~~ the Ti-Ta composite, with hierarchical "brick-and-mortar" microstructure, the yield strength decreases for about 50 MPa after short-time annealing. However, the as-annealed composite shows much higher strain hardening effect than the as-rolled ones. The most reasonable reason is the appearance of nano-scaled precipitations inside the Ta-enriched bands (Fig. 2g), which formed after annealing.

When being applied the uniaxial tensile stress, the slip systems in the Ta-enriched bands first move and plastic deformation occurs. Owing to the "brick-and-mortar" structure, the dislocations first slide inside the relative soft bands which are constrained by interface between R-Ti and R-Ta in Ta-enriched bands. Interestingly, a large amount of Ti-enriched precipitations occur inside the Ta-enriched bands after short-time annealing. The boundaries

of precipitations can also restrict the movement of dislocations inside the Ta-enriched bands. Therefore, the precipitations inside the Ta-enriched bands may have great effect on the back stress. This may lead to the back stress effect, which makes it difficult for dislocations to further slip inside the Ta-enriched band. A much larger strength is acquired to drive dislocation motion with the occurrence of "brick-and-mortar" structure, leading to the "up-turn" in the strain hardening rate, and the similar phenomenon is also shown in other "brick-and-mortar" structured composites. For example, Huang et al. [50] have reported the obvious back stress in Cu/Cu10Zn heterogeneous laminate material which led to both higher strength and higher ductility. Besides, they have suggested that the back-stress work hardening is most effective in the early stage of plastic deformation. Besides, Zhu et al. [51] pointed out that the back stress in the soft phase will also form a forward stress through the interface to the hard phase, and the mechanical behavior of heterostructured materials depends on the interaction of both stress to different phases. The strengthening in such structures thus is called as hetero-deformation induced (HDI) hardening.

From the perspective of composite structures, both strength and ductility are improved after annealing with nano-sized precipitation formations. For conventional metals and alloys, thermal annealing promotes plasticity recovery through dislocation annihilation, hence leading to yield strength reduction. However, This is not the case for our Ti-Ta composite with a hierarchical "brick-and-mortar" microstructure. Its yield strength decreases only slightly by ~50 MPa after short-time annealing., However, the as-annealed composite become stronger than the as-rolled one to retain its strain hardening rate with the plastic flow. Apparently, this could be attributed to the precipitation of Ti-rich phase inside R-Ta, which strengthens the back stress effect in the "brick-and-mortar" microstructure. However, the question is how much the effect of the Ti-rich phase on the witnessed strength-ductility synergy is, and if the overall effect of the "brick-and-mortar" microstructure could be excluded.

~~4.2 Multiple micro-mechanisms~~

Formatted: Indent: First line: 2 ch

The highly improved strength and good ductility of the Ti-Ta composite can be attributed to the following reasons: (1) ~~for one thing,~~ the hierarchical "brick and mortar" structure may lead to the back stress effect, which can obviously improve the strength;. (2) ~~For another,~~ the grain refinement of the Ti-Ta composite can also improve the strength. The fine-scaled α phase inside the Ti-enriched bands, the sub-micro sized elemental distributions in Ta-enriched bands after rolling both can restrict the movement of dislocations, improving

the dislocation density markedly and thus enhancing the strength. Especially for the as-annealed composite, the nano-scale Ti-rich precipitates inside the R-Ta can block the movement of dislocations and thus improve the strength. Therefore, the Ti-Ta composite has a much better combination of strength and ductility than other Ti alloys. Fig.9 concludes the multiple micro-mechanisms of the Ti-Ta composite with "brick-and-mortar" structure. The Ti-enriched bands, consisted of fine-scaled α phase, can block the dislocations and act as "brick" in this special microstructure. As for the relative soft Ta-enriched bands, it is known that SIMT improves ductility by increasing the flow stress in a localized area to restrain the plastic instability. Therefore, they are considered as "mortar" in the composite, coordinating the deformation behaviors of the whole composite. In general, these strain hardening phenomena should be more dependent on nano-precipitation and back stress effects, while the stress induced phase transformation mainly contributes to the ductility.

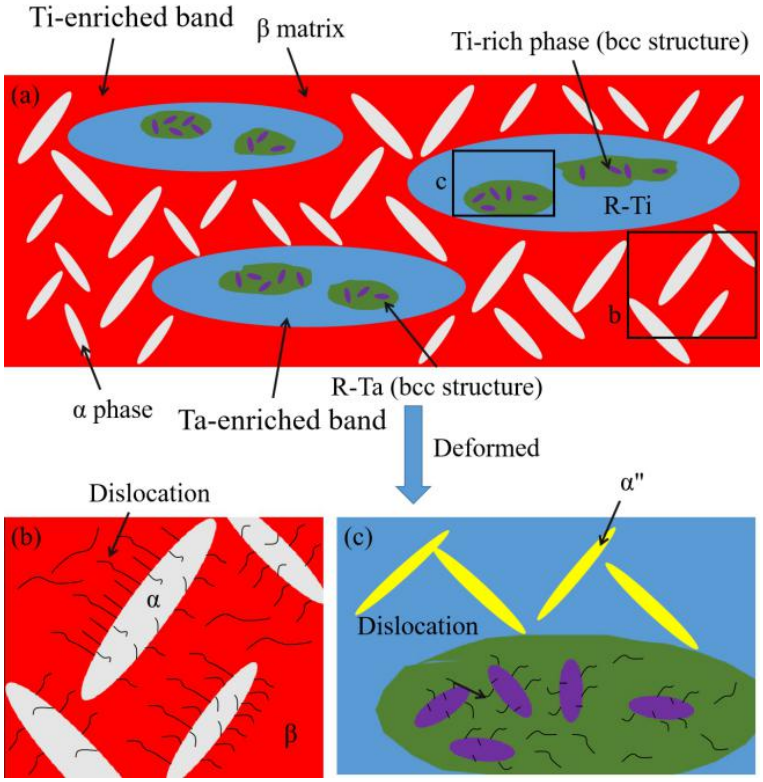

Fig.9 The diagrammatic schematic of the as-annealed Ti-Ta composite: (a) the phase compositions before tensile deformation; (b) and (c) the deformation mechanisms of Ti-enriched and Ta-enriched bands.

5. Conclusions

A novel Ti-Ta based composite with bio-mimic “brick-and-mortar” structure is designed and successfully fabricated through spark plasma sintering, rolling and annealing. The main findings and results are summarized as follows:

1. The microstructure of the Ti-Ta composite is hierarchical with banded structures. Ti-enriched band consists of high-density of nano-size α phase, which is the hard ‘brick’. The soft ‘mortar’ Ta-enriched band consists of two submicron regions rich in Ti and Ta, respectively. Nano precipitates are found within the Ti rich region in the Ta-enriched band after annealing.

2. The Ti-Ta composite at its annealed condition has excellent mechanical performance (1226 MPa ultimate tensile strength and 20.8% elongation), which is attributed to its special hierarchical microstructure.

3. Stress induced martensitic phase transformation ~~(SIMT)~~ was observed by in situ tensile testing under synchrotron x-ray diffraction.

4. The Ti-rich nanoprecipitates formed after annealing can block the movement of dislocations and enhances the overall HDI stress effect in the “brick-and-mortar” microstructure, and thus the Ti-Ta composite has much better combination of strength and ductility than other Ti alloys.

Acknowledgement

The authors gratefully acknowledge the financial support from the National Science Fund for Distinguished Young Scholars (51625404), and the Hunan Natural Science Foundation of China (2017JJ2311). YY acknowledges the support from the financial support from the Research Grant Council, the Hong Kong government, through the general research fund (grant Nos. CityU11207215 and CityU11209317). The authors gratefully acknowledge the use of I12 beamline, Diamond Light Source (DLS) via Beamtime EE18192.

References

[1] S. Feng, Q. Guo, Z. Li, G. Fan, Z. Li, D.B. Xiong, Strengthening and toughening mechanisms in graphene-Al nanolaminated composite micro-pillars, Acta Materialia, 2017(125):98-108.

[2] X. Ma, C. Huang, J. Moering, M. Ruppert, H.W. Höppel, M. Göken, Mechanical properties of copper/bronze laminates: Role of interfaces, Acta Materialia, 2016(116):43-52.

[3] G.S. Pradeep, P.G. Koppa, R. Keshavamurthy, M. Alipour, Microstructure and mechanical behaviour of in situ fabricated AA6061-TiC metal matrix composites, Archives of Civil and Mechanical Engineering, 2017(17):535-544.

[4] N. Sadeghi, H. Aghajani, M.. RAkbarpour, Microstructure and tribological properties of in-situ TiC-C/Cu nanocomposites synthesized using different carbon sources (graphite, carbon nanotube and graphene) in the Cu-Ti-C system. Ceramics International, 2018(44): 22059-22067.

[5] Y. Han, F. Jiang, C. Lin, D. Yuan, H. Huang, E. Wang, Microstructure and mechanical properties of continuous ceramic SiC and shape memory alloy NiTi hybrid fibers reinforced Ti-Al metal-intermetallic laminated composite, Journal of Alloys and Compounds, 2017(729):1145-1155.

[6] A.A. Costa, D. Silva, D.N. Travessa, E.C. Botelho, The effect of thermal cycles on the mechanical properties of fiber–metal laminates, Materials & Design, 2012(42):434-440.

[7] H. Kou, J. Lu, Y. Li, High-Strength and High-Ductility Nanostructured and Amorphous Metallic Materials, Advanced Materials, 2014(26):5518-5524.

[8] X.L. Wu, M. Yang, F. Yuan, G. Wu, Y. Wei, X. Huang, Heterogeneous lamella structure unites ultrafine-grain strength with coarse-grain ductility, Proceedings of the National Academy of Sciences of the United States of America, 2015(112):14501-14505.

[9] F. Cheng, W. Liu, Y. Zhang, H. Wang, S. Liu, E. Hao, Squid inks-derived nanocarbons with unique “shell@pearls” structure for high performance supercapacitors, Journal of Power Sources, 2017(354):116-123.

[10] L.B. Mao, L.G. He, H.B. Yao, L. Liu, H. Cölfen, G. Liu, S.M. Chen, S.K. Li, Y.X. Yan, Y.Y. Liu, S.H. Yu, Synthetic nacre by predesigned matrix-directed mineralization, Science, 2016 (354):107-110.

[11] K.Z. Motomichi, M.M. Wang, D. Ponge, D. Raabe, K. Tsuzaki, H. Noguchi, C.C. Tasan. Bone-like crack resistance in hierarchical metastable nanolaminate steels, Science, 2017(355):1055-1057.

[12] Q. Guo, L. Wan, X.X.Yu, F. Vogel, G.B. Thompson, Influence of phase stability on the in situ growth stresses in Cu/Nb multilayered films, Acta Materialia, 2017(132):149-161.

[13] C.S. Hong, N.R. Tao, X. Huang, K. Lu, Nucleation and thickening of shear bands in nano-scale twin/matrix lamellae of a Cu-Al alloy processed by dynamic plastic deformation, Acta Materialia, 2010(58):3103-3116.

[14] M.E. Launey, E. Munch, D.H. Alsem, H.B. Barth, E. Saiz, A.P. Tomsia, Designing highly toughened hybrid composites through nature-inspired hierarchical complexity, Acta Materialia, 2009(57):2919-2932.

[15] Z.W. Shan, R.K. Mishra, S.A. Asif, O.L. Warren, A.M. Minor, Mechanical annealing and source-limited deformation in submicrometre-diameter Ni crystals, Nature Materials, 2007(7):115.

[16] M. Kashtalyan, Y. Sinchuk, R. Piat, I. Guz, Analysis of multiple cracking in metal/ceramic composites with lamellar microstructure, Archive of Applied Mechanics, 2015(86):177-188.

[17] C. Gaudillere, J.M. Serra, Freeze-casting: Fabrication of highly porous and hierarchical ceramic supports for energy applications, Boletín de la Sociedad Española de Cerámica y Vidrio, 2016(55):45-54.

[18] A.V.Demchishin, I. Gnilitskyi, L. Orazi, A. Ascari, Structure, phase composition and microhardness of vacuum-arc multilayered Ti/Al, Ti/Cu, Ti/Fe, Ti/Zr nano-structures with different periods, Applied Surface Science, 2015(342):127-135.

[19] X.Y. Zhu, X.J. Liu, F. Zeng, F. Pan, Microstructure and nanoindentation hardness of Ag/Fe multilayers, Transactions of Nonferrous Metals Society of China, 2010(20):110-114.

[20] D.W. Wang, Y.H. Zhou, J. Shen, Y. Liu, D.F. Li, Q. Zhou, Selective laser melting under the reactive atmosphere: A convenient and efficient approach to fabricate ultrahigh strength commercially pure titanium without sacrificing ductility, Materials Science and Engineering: A, 2019(762):138078.

[21] Y.H. Zhou, W.P. Li, D.W. Wang, L. Zhang, K. Ohara, J. Shen, Selective laser melting enabled additive manufacturing of Ti-22Al-25Nb intermetallic: Excellent combination of strength and ductility, and unique microstructural features associated, Acta Materialia, 2019(173):117-129.

[22] H. Liu, Z. Li, F. Gao, Y. Liu, Q. Wang, High tensile ductility and strength in the Ti-42Al-6V-1Cr alloy, Journal of Alloys and Compounds, 2017(698):898-905.

[23] K. Yue, J. Liu, H. Zhang, H. Yu, Y. Song, Q. Hu, Precipitates and alloying elements distribution in near α titanium alloy Ti65, Journal of Materials Science & Technology, 2019.

[24] L. Huang, M. Qian, L. Wang, Z.G. Chen, Z. Shi, V. Nguyen, High-tensile-strength and ductile novel Ti-Fe-N-B alloys reinforced with TiB nanowires, Materials Science and Engineering: A, 2017(708):285-290.

[25] Y. Yu, Y.H. Cai, X.H. Chen, T. Wang, Y.D. Wu, J.J. Si, A high strength and elastic carbon containing near-α Ti alloy prepared by hot isostatic pressing process, Materials Science and Engineering: A, 2016(651):961-967.

[26] J. Zhang, J. Li, G. Chen, L. Liu, Z. Chen, Q. Meng, Fabrication and characterization of a novel β metastable Ti-Mo-Zr alloy with large ductility and improved yield strength, Materials Characterization, 2018(139):421-427.

[27] S. Guo, Q. Meng, X. Cheng, X. Zhao, α′ martensite Ti-10Nb-2Mo-4Sn alloy with ultralow elastic modulus and High strength, Materials Letters, 2014(133):236-239.

[28] Q. Guo, Q. Wang, D.L. Sun, X.L. Han, G.H. Wu, Formation of nanostructure and mechanical properties of cold-rolled Ti-15V-3Sn-3Al-3Cr alloy, Materials Science and Engineering: A, 2010(527):4229-4232.

[29] C. Lan, Y. Wu, L. Guo, H. Chen, F. Chen, Microstructure, texture evolution and mechanical properties of cold rolled Ti-32.5Nb-6.8Zr-2.7Sn biomedical beta titanium alloy, Journal of Materials Science & Technology, 2018(34):788-792.

[30] W.D. Zhang, Y. Liu, H. Wu, B. Liu, Z.J. Chen, H.P. Tang, Microstructural evolution during hot and cold deformation of Ti-36Nb-2Ta-3Zr-0.35O alloy, Transactions of Nonferrous Metals Society of China, 2016(26):1310-1316.

[31] P. Neacsu, D.M. Gordin, V. Mitran, T. Gloriant, M. Costache, A. Cimpean, In vitro performance assessment of new beta Ti-Mo-Nb alloy compositions, Materials Science and Engineering: C, 2015(47):105-113.

[32] Y. Shi, G. Zhang, M. Li, D. Guo, Z. Zhang, B. Wei, Effect of heat treatment on the microstructure and tensile properties of deformed α/β Ti-47Zr-5Al-3V alloy, Journal of Alloys and Compounds, 2016(665):1-6.

[33] T.W. Xu, J.S. Li, S.S. Zhang, F.S. Zhang, X.H. Liu, Cold deformation behavior of the Ti-15Mo-3Al-2.7Nb-0.2Si alloy and its effect on α precipitation and tensile properties in aging treatment, Journal of Alloys and Compounds, 2016(682):404-411.

[34] X.J. Jiang, X.Y. Wang, Z.H. Feng, C.Q. Xia, C.L. Tan, S.X. Liang, Effect of rolling temperature on microstructure and mechanical properties of a TiZrAl alloy, Materials Science and Engineering: A, 2015(635):36-42.

[35] Y. Chong, T. Bhattacharjee, N. Tsuji, Bi-lamellar microstructure in Ti-6Al-4V: Microstructure evolution and mechanical properties, Materials Science and Engineering: A, 2019(762):138077.

[36] V.Y. Zadorozhnyy, X. Shi, D.S. Kozak, T. Wada, J.Q. Wang, H. Kato, Electrochemical behavior and biocompatibility of Ti-Fe-Cu alloy with high strength and ductility, Journal of Alloys and Compounds, 2017(707):291-297.

[37] A. Biesiekierski, D. Ping, Y. Li, J. Lin, K.S. Munir, Y.Y. Mitarai, Extraordinary high strength Ti-Zr-Ta alloys through nanoscaled, dual-cubic spinodal reinforcement, Acta Biomaterialia, 2017(53):549-558.

[38] S.H. Xu, C.S. Zhou, Y. Liu, B. Liu, K.Y. Li, Microstructure and mechanical properties of Ti-15Mo-xTiC composites fabricated by in-situ reactive sintering and hot swaging, Journal of Alloys and Compounds, 2018(738):188-196.

[39] M. Hosseini, H.D. Manesh, M. Eizadjou, Development of high-strength, good-conductivity Cu/Ti bulk nano-layered composites by a combined roll-bonding process, Journal of Alloys and Compounds, 2017(701):127-130.

[40] Y. Zhang, X. Cheng, H. Cai, H. Zhang, Effects of annealing time on the microstructures and tensile properties of formed laminated composites in Ti-Ni system, Journal of Alloys and Compounds, 2017(699):695-705.

[41] Y. Shao, D.Q. Jiang, F.M. Guo, Y.D. Ru, X.W. Hu, L.S. Cui, Fabrication and Property of W/Tininb Shape Memory Alloy Laminated Composite, Materials Science Forum, 2015(815):211-216.

[42] H. Wu, G. Fan, B.C. Jin, L. Geng, X. Cui, M. Huang, Fabrication and mechanical properties of TiBw /Ti-Ti(Al) laminated composites, Materials & Design, 2016(89):697-702.

[43] M.X. Yang, Y. Pan, F.P. Yuan, Y.T. Zhu, W.L. X, Back stress strengthening and strain hardening in gradient structure, Materials Research Letters, 2016(4):145-151.

[44] X.L. Wu, Y.T. Zhu, Heterogeneous materials: a new class of materials with unprecedented mechanical properties, Materials Research Letters, 2017(5):527-532.

[45] X. Ma, F. Li, J. Cao, J. Li, Z. Sun, G. Zhu, Strain rate effects on tensile deformation behaviors of Ti-10V-2Fe-3Al alloy undergoing stress-induced martensitic transformation, Materials Science and Engineering: A, 2018(710):1-9.

[46] A. Zafari, K. Xia, Stress induced martensitic transformation in metastable β Ti-5Al-5Mo-5V-3Cr alloy: Triggering stress and interaction with deformation bands, Materials Science and Engineering: A, 2018(724):75-79.

[47] S.H. Xu, Y. Liu, C. Yang, H.L. Zhao, B. Liu, J.B. Li, Compositionally gradient Ti-Ta metal-metal composite with ultra-high strength, Materials Science and Engineering: A, 2018(712):386-393.

[48] A. Ahadi, E. Rezaei, Microstructure and Phase Transformation Behavior of a Stress-Assisted Heat-Treated Ti-Rich NiTi Shape Memory Alloy, Journal of Materials Engineering and Performance, 2011(21):1806-1812.

[49] Y.W. Chai, H.Y. Kim, H. Hosoda, S. Miyazaki, Self-accommodation in Ti-Nb shape memory alloys, Acta Materialia, 2009(57):4054-4064.

[50] C.X. Huang, Y.F. Wang, X.L. Ma, S. Yin, H.W. Höppel, M. Göken, Interface affected zone for optimal strength and ductility in heterogeneous laminate, Materials Today, 2018(21):713-719.

[51] Y.T. Zhu, X.L. Wu, Perspective on hetero-deformation induced (HDI) hardening and back stress, Materials Research Letters, 2019(7): 393-398